

The Single- and Double-Strand Cleavage of DNA by a Cationic Dicobalt Complex by Visible Light

Hisashi Shimakoshi, Takeshi Kaieda, and Yoshio Hisaeda*

Department of Chemistry and Biochemistry, Graduate School of Engineering, Kyushu University, Nishi-ku, Fukuoka 819-0395

Received June 12, 2009; E-mail: yhisatcm@mail.cstm.kyushu-u.ac.jp

A one-pot synthesis of a new polycationic organo–dicobalt complex having dual cationic alkyl groups as radical sources is reported. The complex was characterized by elemental analysis, UV–vis, ^{1}H NMR, IR, and CSI-mass spectroscopies. CSI-MS afforded intact parent ion peak with labile cobalt–carbon bonds in the complex. The complex was photosensitive, and photocleavage of the cobalt–carbon bonds upon irradiation with visible light produced dual cationic carbon-centered radicals that were detected by EPR spin-trapping. Strong binding of the dicobalt complex with six cationic moieties toward DNA was confirmed by ethidium bromide displacement assays with $K_{app} = 3.2 \times 10^7\,M^{-1}$ at 298 K, the value was 100 times that of corresponding monocobalt complex with $K_{app} = 3.3 \times 10^5\,M^{-1}$. The dicobalt complex exhibited high ability for single- and double-strand DNA cleavage in comparison with that for the corresponding monocobalt complex under irradiation with visible light.

Formation and cleavage of a metal–carbon σ-bond are important research targets in organometallic chemistry. Especially, compounds with cobalt–carbon bonds found as key intermediates in B_{12}-dependent enzymic reactions have a storied history in bioinorganic chemistry and have proven to be quite useful as a source of carbon-centered radical species.[1] The cobalt–carbon bond is readily cleaved homolytically by photolysis, electrolysis, and thermolysis to form the corresponding carbon-centered radical species.[2] Thus, the application of compounds with cobalt–carbon bonds to organic synthesis is an area of active interest from both practical and mechanistic perspectives.[2] In the course of this study, a variety of chelated complexes having a cobalt–carbon bond have been synthesized and are used as a versatile radical source for molecular transformation.[2,3] Among the reactions, carbon-centered radical degradation of DNA is of significant interest in the search for antitumor agents, and some alkylcobalt(III) complexes have been utilized for the reaction.[4]

Furthermore, the utility of a dimetallic complex that connects dual radical sources together and enhances single-strand (ss) DNA cleavage has been reported,[5a] and a strategy for design of polymetallic complexes that increase double-strand (ds) DNA scission was shown by Mohler et al.[5b] Because of the increasing quest for new antibiotic and anticancer agents,[6,7] the development of a synthetic metal complex which performs dsDNA cleavage has emerged in last ten years[8] where dsDNA cleavage creates damage that is considered much more difficult for the cell to repair than ssDNA cleavage. Previously, we also reported the syntheses of a dicobalt complexes having two cobalt–carbon bonds as shown in Chart 1,[9] and this complex showed more efficient cleavage of ssDNA than the corresponding monocobalt complex by irradiation with visible light at room temperature.[9b]

Based on this background, we designed a new dicobalt complex **1** which has a cationic radical source upon simultaneous or near-synchronous homolytic cleavage of both cobalt–carbon bonds in response to mild visible light irradiation, as shown in Figure 1. The polycationic dicobalt complex **1** strongly binds to DNA and shows efficient ssDNA and dsDNA cleavage upon exposure to visible light via a putative template reaction.

Experimental

Reagents and Chemicals. All reagents and chemicals were obtained from commercial sources and used as received. 5,5-Dimethyl-1-pyrroline *N*-oxide (DMPO) and 4-hydroxy-2,2,6,6-tetramethylpiperidine 1-oxyl (HTEMPO) were purchased from Tokyo Chemical Industry (TCI, Japan). Dimethyl sulfoxide (biotech. grade) was obtained from Nacalai Tesque (Japan). Superoxide dismutase (SOD enzyme) was purchased from Cosmo Bio (Japan). 3,3′,4,4′-Tetraaminodiphenylmethane, 5-(trimethylammoniomethyl)salicylaldehyde chloride, and bromomethyltrimethylammonium bromide were synthesized as described in the literature.[10–12] Plasmid DNA pBR322 (4361 bp) and ethidium bromide (EtBr) were purchased from Nippon Gene (Japan) and Aldrich, respectively. Loading buffer and *Eco*R 1 were purchased from Takara Bio (Japan). Calf thymus DNA was purchased from Sigma. Distilled, deionized water from a Milli-Q system was used for all aqueous solutions and manipulations.

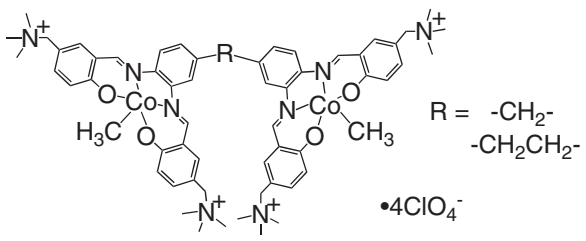

Chart 1.

Published on the web November 10, 2009; doi:10.1246/bcsj.82.1386

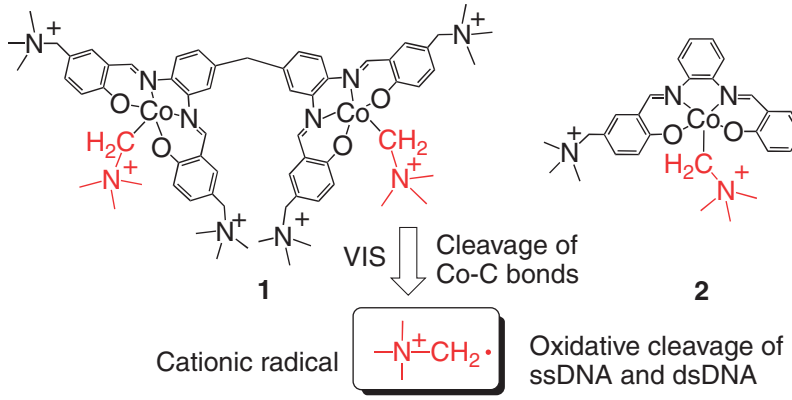

Figure 1. Molecular structures of cationic alkylated cobalt complexes.

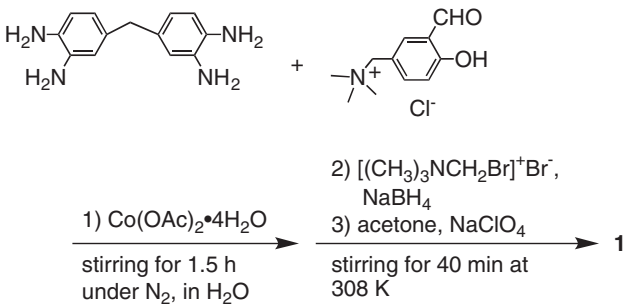

Scheme 1. Synthesis of dialkylated dicobalt complex **1**.

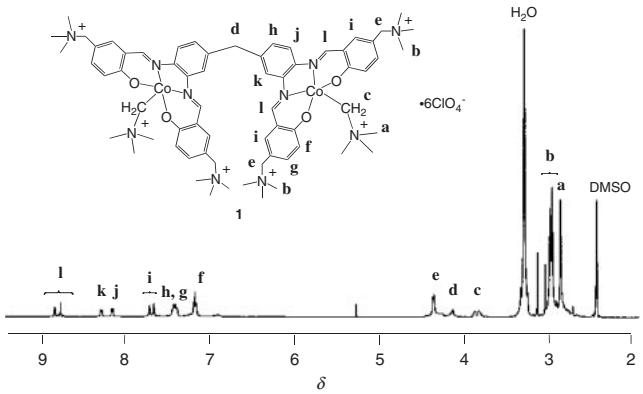

Figure 2. ^{1}H NMR spectrum (500 MHz, in DMSO-d_6) of **1**. The assignments are shown in the figure.

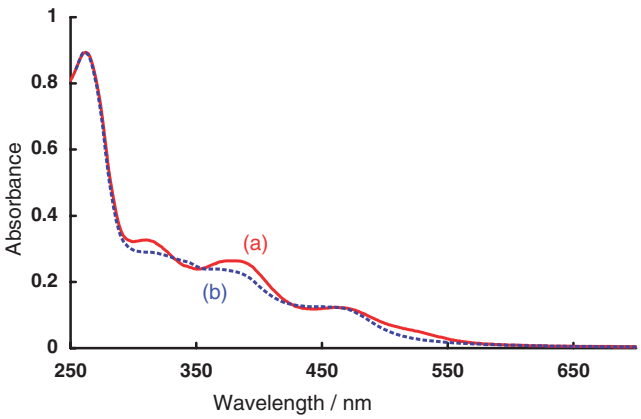

Figure 3. Electronic spectral change for the aerobic photolysis of **1**: (a) in TBE buffer; (b) after irradiation with visible light (500-W tungsten lamp, cutoff filter $\lambda \geq 410$ nm).

Instrumentations. The elemental analyses were obtained from the Service Center of Elementary Analysis of Organic Compounds at Kyushu University. The ^{1}H, ^{13}C, and COSY NMR spectra were recorded with a Bruker Avance 500 spectrometer installed at the Center of Advanced Instrumental Analysis at Kyushu University, and the chemical shifts (δ) were referenced relative to the residual protic solvent peak. The UV–vis absorption spectra were measured using a Hitachi U-3300 spectrophotometer at room temperature. The IR spectra were recorded on a JASCO FT-IR 460 plus KH spectrophotometer using KBr discs. The CryoSpray ionization (CSI)-TOF mass spectra were obtained with a bruker micrOTOF in MeOH–H_2O (1:1, v/v) at 273 K. The fluorescence spectra were measured with a Hitachi F-4500. The pH values were monitored with a Beckman Φ 71 pH meter.

Synthesis of Dicobalt Complex 1 (Scheme 1). To a degassed H_2O (35 mL) solution of 3,3′,4,4′-tetraaminodiphenylmethane (45.6 mg, 0.2 mmol) and 5-(trimethylammoniomethyl)salicylaldehyde chloride (183.9 mg, 0.8 mmol) was added $Co(OAc)_2 \cdot 4H_2O$ (99.9 mg, 0.4 mmol). After the solution was stirred for 1.5 h under nitrogen atmosphere at room temperature, bromomethyltrimethylammonium bromide (0.979 g, 4.20 mmol) and $NaBH_4$ (98.5 mg, 2.6 mmol) were added to it and stirred for 40 min at 308 K in the dark. The excess $NaBH_4$ was decomposed with acetone (2 mL), followed by the addition of 3.3 M $NaClO_4$ aqueous solution (10 mL), and the solution was kept at 278 K for 1 h to precipitate a dark-brown powder. The powder was washed with a small amount of MeOH and Et_2O and dried in vacuo in the dark. Recrystallization from DMF–MeOH/Et_2O gave compound **1**. Yield: 89 mg (53%). UV–vis (in TBE buffer): [λ_{max}/nm (ε)], 262 (91200), 310 (33400), 380 (27000). CSI-MS (TOF): m/z $(M - 2ClO_4)^{2+}$, 794.1; $(M - 3ClO_4)^{3+}$, 496.4. Anal. Found: C, 43.75; H, 5.30; N, 7.63%. Calcd for $C_{65}H_{90}N_{10}Cl_6Co_2O_{28}$: C, 43.61; H, 5.07; N, 7.82%. ^{1}H NMR (DMSO-d_6): δ 2.91 (s, 18H, –NCH_3), 3.01 (s, 18H, –NCH_3), 3.04 (s, 18H, –NCH_3), 3.86–3.92 (m, 4H, Co–CH_2NCH_3), 4.18 (s, 2H, Ph–CH_2–Ph), 4.40 (s, 4H, –CH_2NCH_3), 4.42 (s, 4H, –CH_2NCH_3), 7.20 (t, J = 8.9 Hz, 4H, Ph), 7.41–7.47 (m, 6H, Ph), 7.69 (s, 2H, Ph), 7.75 (s, 2H, Ph), 8.17 (d, J = 8.8 Hz, 2H, Ph), 8.30 (d, J = 8.8 Hz, 2H, Ph), 8.79 (s, 2H, imine), 8.87 (s, 2H, imine). IR, ν/cm^{-1}: 1617 (C=N, str.), 1335 (C–O, str.), 1143, 1108, 1089 (ClO_4^-, str.). The ^{1}H NMR and UV–vis spectra of **1** are shown in Figures 2 and 3, respectively.

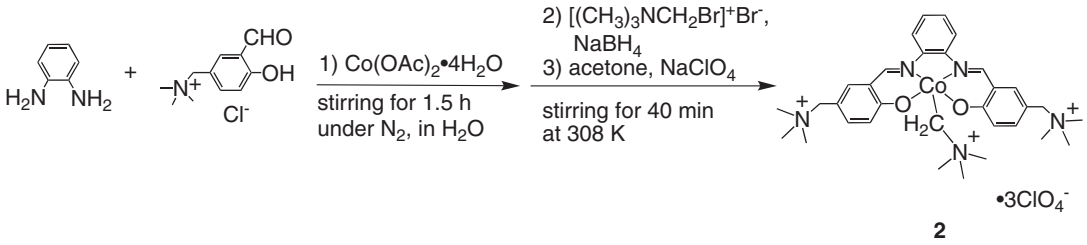

Scheme 2. Synthesis of monoalkylated monocobalt complex **2**.

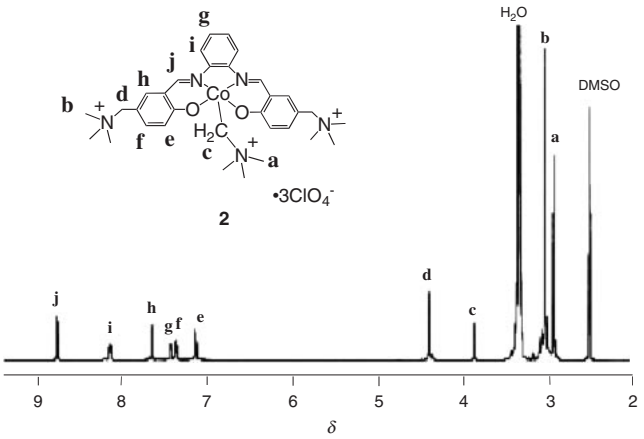

Figure 4. ^{1}H NMR spectrum (500 MHz, in DMSO-d_6) of **2**. The assignments are shown in the figure.

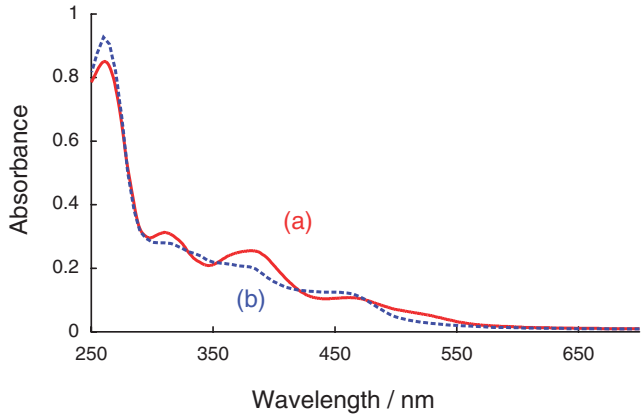

Figure 5. Electronic spectral change for the aerobic photolysis of **2**: (a) in TBE buffer; (b) after irradiation with visible light (500-W tungsten lamp, cutoff filter $\lambda \geq 410$ nm).

Synthesis of Monocobalt Complex 2 (Scheme 2). To a degassed H_2O (35 mL) solution of *o*-phenylenediamine (86.5 mg, 0.8 mmol) and 5-(trimethylammoniomethyl)salicylaldehyde chloride (367.8 mg, 1.6 mmol) was added $Co(OAc)_2 \cdot 4H_2O$ (200.7 mg, 0.81 mmol). After the solution was stirred for 1.5 h under nitrogen atmosphere at room temperature, bromomethyltrimethylammonium bromide (745.4 mg, 3.20 mmol) and $NaBH_4$ (151.9 mg, 4.02 mmol) were added and the mixture was stirred for 40 min at 308 K in the dark. The excess $NaBH_4$ was decomposed with acetone (2 mL), followed by the addition of 3.3 M $NaClO_4$ aqueous solution (5 mL), and the solution was kept at 278 K for 12 h to precipitate a dark-brown powder. The powder was washed with MeOH and dried in vacuo in the dark. Yield: 177.8 mg (25%). UV–vis (in TBE buffer): [λ_{max}/nm (ε)], 261 (49000), 310 (17800), 381 (14400). CSI-MS (TOF): m/z $(M - ClO_4)^+$, 788.1. Anal. Found: C, 43.15; H, 5.22; N, 7.77%. Calcd for $C_{32}H_{45}N_5Cl_3Co_1O_{14}$: C, 43.23; H, 5.10; N, 7.88%. ^{1}H NMR (DMSO-d_6): δ 2.91 (s, 9H, –NCH_3), 3.01 (s, 18H, –NCH_3), 3.87 (s, 2H, Co–CH_2NCH_3), 4.41 (s, 4H, –CH_2NCH_3), 7.19 (d, $J = 8.7$ Hz, 2H, Ph), 7.42 (d, $J = 8.7$ Hz, 2H, Ph), 7.48 (dd, $J = 7.5$ Hz, 3.1 Hz, 2H, Ph), 7.71 (s, 2H, Ph), 8.12 (dd, $J = 6.0$ Hz, 3.3 Hz, 2H, Ph), 8.86 (s, 2H, imine). IR, ν/cm^{-1}: 1616 (C=N, str.), 1336 (C–O, str.), 1144, 1110, 1088 (ClO_4^-, str.). The ^{1}H NMR and UV–vis spectra of **2** are shown in Figures 4 and 5, respectively.

Plasmid DNA Cleavages. The DNA cleavage activities of the complexes were studied by agarose gel electrophoresis. Supercoiled pBR322 DNA (200 μM) in TBE buffer (pH 8.4) was treated with the complexes **1** and **2**. The solutions were equilibrated in the dark for 1 h and were then irradiated with visible light (500-W tungsten lamp) through a cutoff filter ($\lambda \geq 410$ nm) for 10 min under aerobic condition. Samples were incubated at 278 K in a loading buffer solution for 2 h and then loaded on 1.0% agarose gel. Electrophoreses were carried out at 50 V for 2 h in TBE buffer. Bands were visualized by UV light (UV Benchtop Transilluminator, TM-10E) and photographed (Polaroid camera, DS-300) after immersion in ethidium bromide solution (0.5 μg mL^{-1}) for 20 min as shown in Figure 6. The concentration dependences of **2** and **1** for DNA strand cleavage were carried out in a similar manner and the results are shown in Figures 7 and 8 for **2** and **1**, respectively.

Plasmid Assay Quantitation Data. Gels were quantified using the software program Total Lab 2.01. The intensities of supercoiled DNA were corrected by a factor of 1.22 as a result of its lower staining capacity by ethidium bromide.

Ethidium Bromide Displacement Assays. The fluorescence intensity of ethidium bromide was determined at an excitation wavelength of 540 nm and an emission wavelength of 590 nm. Ethidium bromide (1.26 μM) and calf thymus DNA (4.0 μM/bp) were dissolved in TBE buffer (pH 8.1, NaCl 10 mM). The fluorescence intensity was recorded after the addition of each concentration of complex at 298 K. The fluorescence spectral changes with the addition of **1** and **2** are shown in Figures 9 and 10, respectively. The apparent binding constants (K_{app}) for **1** and **2** were determined by the following equation: K_{EtBr}[EtBr] = K_{app}[complex]. In the equation, [complex] is the concentration of the alkylated cobalt complex at 50% decrease in fluorescence of ethidium bromide. The binding constant of ethidium bromide to calf thymus DNA, $K_{EtBr} = 4.3 \times 10^6$ M^{-1} under the condition used was determined by a reported method[13] using the McGhee–von Hippel equation.[14]

EPR Spectroscopy. The EPR spectra were obtained on a JEOL JES-FE1G X-band spectrometer equipped with an Advantest TR-5213 microwave counter and an Echo Electronics EFM-

200 NMR field meter. The typical settings for the EPR spectra were: frequency 9.45 GHz, power 1 mW, sweep width 100 G, center field 3365 G, sweep time 8 min, time constant 0.1 s, modulation frequency 100 kHz, modulation width 1.6 G, gain 500. The EPR spectra observed after photolysis (500-W tungsten lamp, $\lambda \geq 410$ nm, 1 min) of alkylated complex **1** (1.0 mM in TBE buffer, pH 8.4) in the presence of DMPO (3.3×10^{-1} M) were obtained under air and oxygen (bubbling for 5 min) at room temperature. EPR simulation was performed with the WINSIM implementation of PEST. The software is available free of charge via the Internet at http://EPR.niehs.nih.gov/pest.html (NIEHS).

Results and Discussion

Synthesis. The complex **1** was synthesized by the following one-pot procedure as shown in Scheme 1. As for **1**, a condensation reaction between 3,3′,4,4′-tetraaminodiphenylmethane and 5-(trimethylammoniomethyl)salicylaldehyde chloride in the presence of $Co(OAc)_2 \cdot 4H_2O$ and the subsequent reaction with $NaBH_4$ and bromomethyltrimethylammonium bromide yield the photo-labile alkylated complex. The complex was characterized by IR, NMR, UV–vis, CSI-MS, and elemental analysis. In the IR spectrum, a band assignable to the C=N vibration of the coordinated azomethine group appeared at 1617 cm^{-1} as shown in Figure S1. The diamagnetic Co^{III} complex **1** shows a well-defined ^1H NMR spectrum as shown in Figure 2. A peak for the imino protons of **1** appeared at 8.79 and 8.87 ppm with 4H integration. The methylenes coordinating to the cobalt centers appeared at 3.89 ppm with 4H integration. On the basis of these numbers, two equivalents of the trimethylammonium methyl group existed in **1**. The presence of labile cobalt–carbon bonds in **1** is also confirmed by the UV–vis spectrum, which shows absorptions at 262, 310, 380, and 470 nm in H_2O (TBE buffer) as shown in Figure 3. This spectrum changed upon irradiation with visible light (Figure 3b), which is characteristic of the cleavage of the cobalt–carbon bonds. Convincing evidence for the dual cobalt–carbon bonds structure of **1** was provided by CSI-MS as shown in Figure S2. The CSI-MS showed intense peaks at m/z 794.1 and 496.4 ascribed to $[\mathbf{1} - 2ClO_4]^{2+}$ and $[\mathbf{1} - 3ClO_4]^{3+}$, respectively, and those satisfied the isotope patterns as shown in Figures S3 and S4. These spectral data strongly suggested the successful preparation of the desired dicobalt complex with dual cobalt–carbon bonds. The referenced monometallic complex **2** was also synthesized as shown in Scheme 2 and was characterized by IR, NMR (Figure 4), UV–vis (Figure 5), CSI-MS, and elemental analysis.

DNA Cleavage. The DNA cleavage activity of **1** was studied using supercoiled plasmid DNA (form I). The complex **1** was photolyzed by a tungsten lamp through a cutoff filter ($\lambda \geq 410$ nm) for 10 min in the presence of pBR322 DNA at room temperature in TBE buffer (pH 8.4), and the amounts of strand scission were assessed by agarose gel electrophoresis as shown in Figure 6. In the case of the dimetallic complex **1** with two cobalt–carbon bonds, a band ascribed to linear DNA (form III) formed by double-strand cleavage of supercoiled plasmid DNA as well as a band for nicked circular DNA (form II) resulting from single-strand cleavage was observed under mild visible light irradiation (lane 5 in Figure 6), while no DNA scission was observed when the sample was simply exposed to visible light in the absence of **1** (lane 2 in Figure 6) or when it was kept in the dark even though **1** was present (lane 3 in Figure 6). The ability of **1** to cleave plasmid DNA was compared to that for the monometallic complex **2** (lane 4 in Figure 6). The amount of double-strand scission was enhanced by the template effect of **1** though the scission ability of **2** was improved due to the cationic radical source compared to that of the previous simple methylated complex which affords a charge-neutral methyl radical.[9b] In the cases of previous complexes, both dicobalt (Chart 1) and monocobalt complexes, formation of linear DNA (form III) was not observed.[9b] Therefore, having cationic charge at a radical moiety should enhance DNA scission ability of the alkylated complex. The template effect of **1** was also confirmed by fact that a band corresponding to form III DNA reached a ceiling at only 2% of the total amount of DNA forms with complex **2** concentrations from 115 to 334 μM as shown in Figure 7. It is necessary that a second strand break occurs on the opposite DNA strand within 16 nucleotides of an initial strand break to form linear DNA by a non-random dsDNA break.[8c] In that

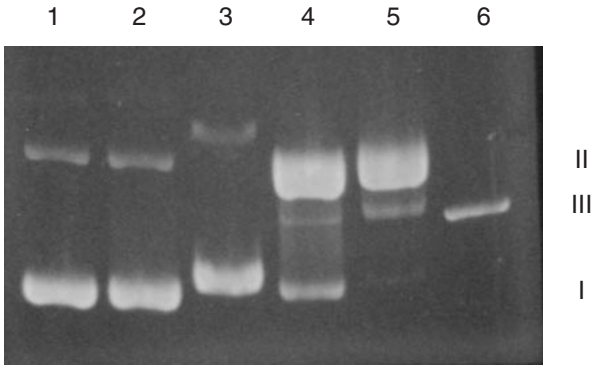

Figure 6. Gel-electrophoretic analysis of strand breaks generated in the photolysis (500-W tungsten lamp, $\lambda \geq 410$ nm, room temperature, 10 min) of supercoiled pBR322 DNA (200 μM/bp in TBE buffer, pH 8.4) in the presence of the alkylated complex. Lane 1, DNA alone (control); lane 2, in the absence of the complex; lane 3, **1** (75 μM) in the dark; lane 4, **2** (150 μM); lane 5, **1** (75 μM); lane 6, form III marker from *Eco*R I (quantitated in Table S1).

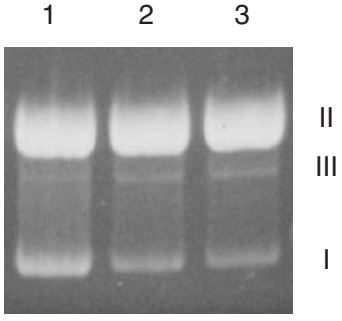

Figure 7. Gel-electrophoretic analysis of supercoiled pBR322 DNA (200 μM/bp in TBE buffer, pH 8.4) treated with different concentrations of **2** after photolysis (500-W tungsten lamp, $\lambda \geq 410$ nm, room temperature, 10 min). Lane 1, **2** 115 μM; lane 2, **2** 230 μM; lane 3, **2** 334 μM (quantitated in Table S2).

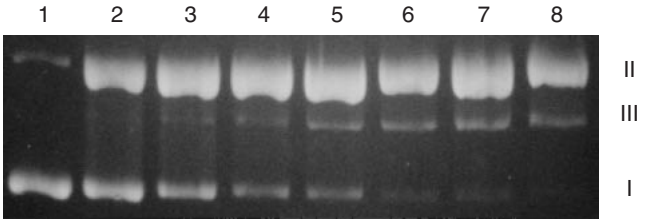

Figure 8. Gel-electrophoretic analysis of supercoiled pBR322 DNA (200 μM/bp in TBE buffer, pH 8.4) treated with different concentrations of **1** after photolysis (500-W tungsten lamp, $\lambda \geq 410$ nm, room temperature, 10 min). Lane 1, DNA alone; lane 2, **1** 25 μM; lane 3, **1** 51 μM; lane 4, **1** 75 μM; lane 5, **1** 101 μM; lane 6, **1** 134 μM; lane 7, **1** 150 μM; lane 8, **1** 176 μM (quantitated in Table S3).

case, the template effect of **1** to form the active species within a desirable range on the DNA presumably causes the dsDNA break.

Furthermore, the minimum concentration of **1** that causes the double-strand break is 51 μM or 0.26 molecules/bp (Figure 8). This value was lower than that of natural enediyne dynemicin A; its value was reported as 0.75 molecules/bp.[15] It is reasonable to suggest that the high cleavage efficiency of complex **1** may arise from the enhanced level of DNA binding confirmed by the apparent binding constant, K_{app}. The K_{app} determined by ethidium bromide (EtBr) displacement assay for **1** was 100 times that of **2** (3.2×10^7 vs. 3.3×10^5 M^{-1}, respectively) (Figures 9 and 10). Strong binding of **1** to plasmid DNA and subsequent simultaneous or near-synchronous formation of dual cationic radical species should allow an efficient dsDNA break.

The origin of linear DNA, arising from successive random single-strand breaks or from a real double-strand break, was elucidated by the statistical test of Povirk et al.[16] that has been used to assay bleomycin and calicheamicin double-strand cleavage.[17] The ratio of single- to double-strand breaks (n_1/n_2) in the case of **1** was 25, which was significantly lower than that expected from the coincidences of random single-strand breaks in a plasmid of this size, where n_1/n_2 is 166.[18] This experiment strongly suggests that most of form III DNA arise from double-strand breaks of form I DNA.

Mechanism of DNA Cleavage. The mechanistic studies of the DNA cleavage reactions were carried out using inhibiting reagents such as 4-hydroxy-2,2,6,6-tetramethylpiperidine 1-oxyl (HTEMPO), DMSO, and superoxide dismutase (SOD enzyme). The HTEMPO, a carbon- and oxygen-centered radical trap, inhibited the reaction (lane 2 in Figure 11), and the hydroxyl radical scavenger DMSO[19] (lane 3 in Figure 11) and superoxide scavenger SOD (lane 4 in Figure 11) do not show any significant effect on the photocleavage activity. Therefore, the carbon-centered radical or the oxyl radical species generated from the carbon-centered radical with oxygen causes the oxidative break in DNA under irradiation with visible light to **1**.

The formation and possible participation in DNA cleavage of a radical species was also confirmed by spin-trapping experiments using 5,5-dimethyl-1-pyrroline *N*-oxide (DMPO). The EPR spectrum for the carbon-centered radical trapped

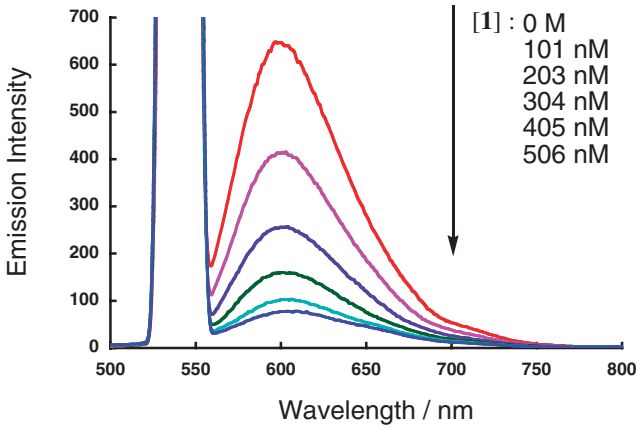

Figure 9. Fluorescence spectral traces of ethidium bromide (1.26 μM in TBE buffer, pH 8.4, NaCl 10 mM) at 298 K in the presence of calf thymus DNA (4.0 μM/bp) showing a decrease in intensity at 590 nm (excitation wavelength: 540 nm) with the addition of **1** (0, 101, 203, 304, 405, and 506 nM).

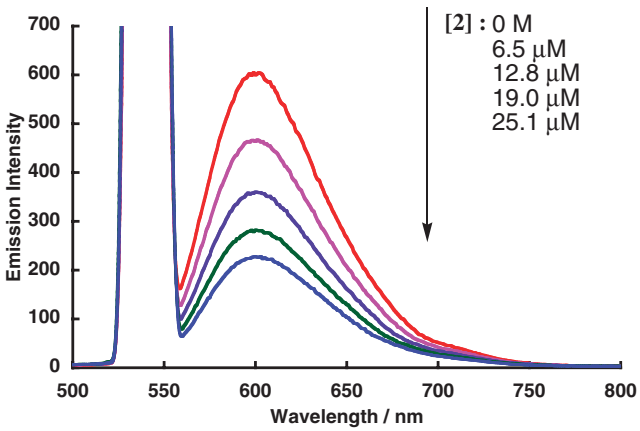

Figure 10. Fluorescence spectral traces of ethidium bromide (1.26 μM in TBE buffer, pH 8.4, NaCl 10 mM) at 298 K in the presence of calf thymus DNA (4.0 μM/bp) showing a decrease in intensity at 590 nm (excitation wavelength: 540 nm) with the addition of **2** (0, 6.5, 12.8, 19.0, and 25.1 μM).

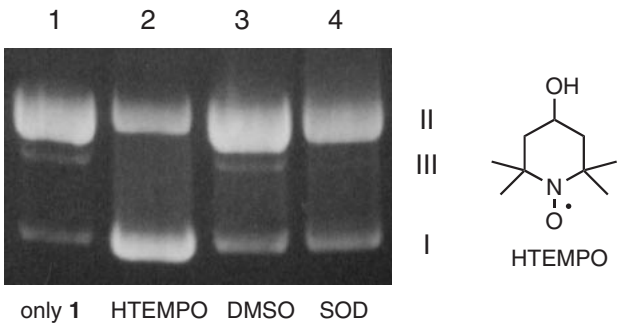

Figure 11. Inhibition studies on cleavage of supercoiled pBR322 DNA (200 μM/bp in TBE buffer, pH 8.4) by **1** (63 μM). Reactions were carried out for 10 min as described in the caption below Figure 6. Lane 1, without inhibitor; lane 2, +100 mM HTEMPO; lane 3, +1 M DMSO; lane 4, +2000 unit/mL SOD (quantitated in Table S4).

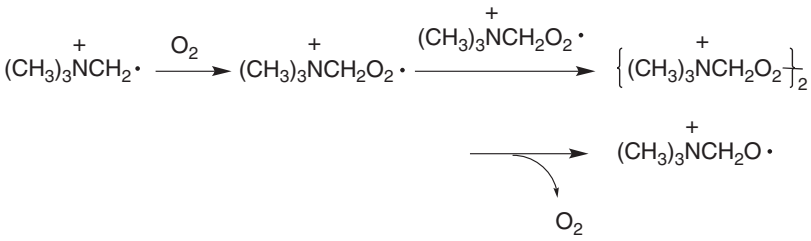

Scheme 3.

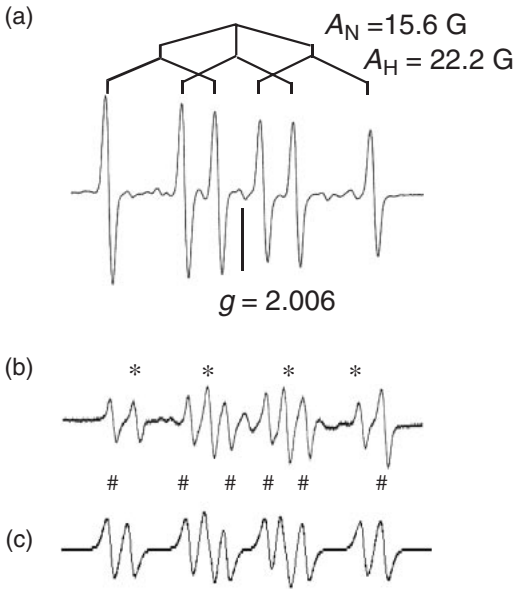

Figure 12. EPR spectra observed in the photolysis (500-W tungsten lamp, $\lambda \geq 410$ nm, 1 min) of **1** (1.0 mM in TBE buffer, pH 8.4) in presence of DMPO (0.33 M): (a) under air, (b) after bubbling oxygen before photolysis; #: carbon-centered radical, ∗: oxygen-centered radical, (c) simulation of spectrum (b).

DMPO ($g = 2.006$, $A_N = 15.6$ G, $A_H = 22.2$ G) was observed with the photolysis of **1** under air as shown in Figure 12a. The hyperfine coupling constants were consistent with those for reported carbon-centered radical trapped DMPO spin adduct ($A_N = 14$–16 G, $A_H = 22$–23 G).[21] A controlled experiment of photolysis **1** under oxygen affords a spectrum combined with those of carbon- and oxygen-centered (alkoxyl) radical trapped species ($A_N = 15.5$ G, $A_H = 22.7$ G and $A_N = 14.9$ G, $A_H = 16.0$ G, respectively) as shown in Figure 12b. Alkyl radicals react with O_2 rapidly to form peroxyl radicals and the rate constant for this reaction is generally of the order of $10^9\,M^{-1}\,s^{-1}$.[22] Thus, according to these experiments, we could not confirm that which radicals, primary formed carbon-centered radical or alkoxyl radical derived from peroxyl radical (Scheme 3), attack DNA for cleavage. Recently, Mohler et al. reported probable participation of alkyl radical for direct DNA cleavage derived from methylated molybdenum complex with strong DNA affinity ($K_{app} = 8.55 \times 10^6\,M^{-1}$).[23,24] Methyl radical generated from photolysis of methylcobalamine induces direct DNA strand break was also proposed by Fukuzumi et al.[4c] Therefore it is possible that the carbon-centered radical also attacks DNA in the reaction used based on strong DNA affinity of **1** ($K_{app} = 3.2 \times 10^7\,M^{-1}$) combined with EPR spin-trapping experiments (Figure 12a). Further study for clarifying the mechanism is needed and is still in progress.

Conclusion

In conclusion, the use of the organo–dicobalt complex with dual cationic alkyl groups as radical sources to achieve ssDNA and dsDNA cleavage has been demonstrated for the first time. The dual cobalt–carbon bonds in the complex increased the ratio of dsDNA cleavage due to its assembly structure. Extensions of the template effect on dicobalt complexes to chemical reaction are currently being pursued in the author's laboratory.

We thank Bruker Daltonics K. K. for measurements of the CSI-MS. This study was partially supported by the Global COE Program "Science for Future Molecular Systems" and Grant-in-Aid for Scientific Research on Priority Areas (460) "Chemistry of Concerto Catalysis" from the Ministry of Education, Culture, Sports, Science and Technology (MEXT) of Japan and Grant-in-Aid for Scientific Research (A) (No. 21245016) from the Japan Society for the Promotion of Science (JSPS).

Supporting Information

IR and CSI-MS of **1** and Table for DNA photocleavage data. This material is available free of charge on the Web at: http://www.csj.jp/journals/bcsj/.

References

1 a) *B_{12}*, ed. by D. Dolphin, Wiley, New York, **1982**. b) J. Halpern, *Science* **1985**, *227*, 869. c) J. M. Pratt, *Pure Appl. Chem.* **1993**, *65*, 1513. d) *Vitamin B_{12} and B_{12}-Protein*, ed. by B. Kräutler, D. Arigoni, B. T. Golding, Wiley-VCH, Weinheim, **1998**. e) *Chemistry and Biochemistry of B_{12}*, ed. by R. Banerjee, Wiley-Interscience, New York, **1999**. f) R. Banerjee, S. W. Ragsdale, *Annu. Rev. Biochem.* **2003**, *72*, 209. g) B. Kräutler, S. Ostermann, in *The Porphyrin Handbook*, ed. by K. M. Kadish, K. M. Smith, R. Guilard, Academic Press, New York, **2003**, *11*, 229. h) K. L. Brown, *Chem. Rev.* **2005**, *105*, 2075.

2 a) R. Scheffold, G. Rytz, L. Walder, R. Orlinski, Z. Chilmonczyk, *Pure Appl. Chem.* **1983**, *55*, 1791. b) I. Das, S. Chowdhury, K. Ravikumar, S. Roy, B. D. Gupta, *J. Organomet. Chem.* **1997**, *532*, 101. c) Y. Hisaeda, T. Nishioka, Y. Inoue, K. Asada, T. Hayashi, *Coord. Chem. Rev.* **2000**, *198*, 21.

3 a) G. N. Schrauzer, J. W. Sibert, R. J. Windgassen, *J. Am. Chem. Soc.* **1968**, *90*, 6681. b) G. Costa, *Coord. Chem. Rev.* **1972**, *8*, 63. c) P. J. Toscano, L. G. Marzilli, *Prog. Inorg. Chem.* **1984**, *31*,

105. d) J. Shey, C. M. McGinley, K. M. McCauley, A. S. Dearth, B. T. Young, W. A. van der Donk, *J. Org. Chem.* **2002**, *67*, 837. e) C. N. McGinley, H. A. Relyea, W. A. van der Donk, *Synlett* **2006**, 211. f) P. Du, M. S. Mubarak, J. A. Karty, D. G. Peters, *J. Electrochem. Soc.* **2007**, *154*, F231.

4 a) C. G. Riordan, P. Wei, *J. Am. Chem. Soc.* **1994**, *116*, 2189. b) M. Vol'pin, I. Levitin, S. Osinsky, *Angew. Chem., Int. Ed. Engl.* **1996**, *35*, 2395. c) M. Tanaka, K. Ohkubo, S. Fukuzumi, *J. Photochem. Photobiol., A* **2008**, *197*, 94.

5 a) D. L. Mohler, J. G. Coonce, D. Predecki, *Bioorg. Med. Chem. Lett.* **2003**, *13*, 1377. b) A. L. Hurley, D. L. Mohler, *Org. Lett.* **2000**, *2*, 2745.

6 a) G. Pratviel, J. Bernadou, B. Meunier, *Angew. Chem., Int. Ed. Engl.* **1995**, *34*, 746. b) C. J. Burrows, J. G. Muller, *Chem. Rev.* **1998**, *98*, 1109.

7 a) T. D. Mody, J. L. Sessler, *J. Porphyrins Phthalocyanines* **2001**, *5*, 134. b) J. L. Sessler, L. R. Eller, W.-S. Cho, S. Nicolaou, A. Aguilar, J. T. Lee, V. M. Lynch, D. J. Magda, *Angew. Chem., Int. Ed.* **2005**, *44*, 5989.

8 a) F. V. Pamatong, C. A. Detmer, III, J. R. Bocarsly, *J. Am. Chem. Soc.* **1996**, *118*, 5339. b) M. S. Melvin, J. T. Tomlinson, G. R. Saluta, G. L. Kucera, N. Lindquist, R. A. Manderville, *J. Am. Chem. Soc.* **2000**, *122*, 6333. c) M. E. Branum, A. K. Tipton, S. Zhu, L. Que, Jr., *J. Am. Chem. Soc.* **2001**, *123*, 1898. d) T. A. van den Berg, B. L. Feringa, G. Roelfes, *Chem. Commun.* **2007**, 180. e) J. He, P. Hu, Y.-J. Wang, M.-L. Tong, H. Sun, Z.-W. Mao, L.-N. Ji, *Dalton Trans.* **2008**, 3207. f) S. Özalp-Yaman, P. de Hoog, G. Amadei, M. Pitié, P. Gamez, J. Dewelle, T. Mijatovic, B. Meunier, R. Kiss, J. Reedijk, *Chem.—Eur. J.* **2008**, *14*, 3418. g) M. Roy, T. Bhowmick, R. Santhanagopal, S. Ramakumar, A. R. Chakravarty, *Dalton Trans.* **2009**, 4671. h) A. K. Patra, T. Bhowmick, S. Roy, S. Ramakumar, A. R. Chakravarty, *Inorg. Chem.* **2009**, *48*, 2932. i) R. P. Megens, T. A. van der Berg, A. D. de Bruijn, B. L. Feringa, G. Roelfes, *Chem.—Eur. J.* **2009**, *15*, 1723. j) M. Cunningham, A. McCrate, M. Nielsen, S. Swavey, *Eur. J. Inorg. Chem.* **2009**, 1521.

9 a) H. Shimakoshi, A. Goto, Y. Tachi, Y. Naruta, Y. Hisaeda, *Tetrahedron Lett.* **2001**, *42*, 1949. b) H. Shimakoshi, T. Kaieda, T. Matsuo, H. Sato, Y. Hisaeda, *Tetrahedron Lett.* **2003**, *44*, 5197. c) H. Shimakoshi, S. Hirose, M. Ohba, T. Shiga, H. Okawa, Y. Hisaeda, *Bull. Chem. Soc. Jpn.* **2005**, *78*, 1040.

10 V. L. Bell, R. A. Jewell, *J. Polym. Sci., Part A: Polym. Chem.* **1967**, *5*, 3043.

11 T. Tanaka, K. Tsurutani, A. Komatsu, T. Ito, K. Iida, Y. Fujii, Y. Nakano, Y. Usui, Y. Fukuda, M. Chikira, *Bull. Chem. Soc. Jpn.* **1997**, *70*, 615.

12 B. Almarzoqi, A. V. George, N. S. Isaacs, *Tetrahedron* **1986**, *42*, 601.

13 B. C. Baguley, E.-M. Falkenhaug, *Nucleic Acids Res.* **1978**, *5*, 161.

14 J. D. McGhee, P. H. von Hippel, *J. Mol. Biol.* **1974**, *86*, 469.

15 T. Shiraki, Y. Sugiura, *Biochemistry* **1990**, *29*, 9795.

16 a) L. F. Povirk, W. Wübker, W. Köhnlein, F. Hutchinson, *Nucleic Acids Res.* **1977**, *4*, 3573. b) L. F. Povirk, C. W. Houlgrave, *Biochemistry* **1988**, *27*, 3850.

17 J. Drak, N. Iwasawa, S. Danishefsky, D. M. Crothers, *Proc. Natl. Acad. Sci. U.S.A.* **1991**, *88*, 7464.

18 Mohler et al. reported in Ref. 5b as follows: The expected n_1/n_2 was determined with the Freifelder–Trumbo equation $n_2 = n_1^2(2h + 1)/4L$ where h is the maximum separation in base pairs between two cuts on complementary strands that produces a linear DNA molecule ($h = 16$), and L is the number of phosphoester bonds per DNA strand in the plasmid ($L = 4361$ for pBR 322), and n_1 and n_2 are the number of single-strand and double-strand DNA cuts, respectively. D. Freifelder, B. Trumbo, *Biopolymers*, **1969**, *7*, 681.

19 DMSO actually traps hydroxyl radical to form methyl radical instead. C. Giulivi, A. Boveris, E. Cadenas, *Arch. Biochem. Biophys.* **1995**, *316*, 909. Thus participation of the methyl radical derived from hydroxyl radical in the reaction was not denied by this experiment. However no existence of hydroxyl radical was confirmed by DMPO spin-trapping experiment as shown in Figure 12a since DMPO–OH show distinct hyperfine splitting parameter ($A_N = 14.7$–15.2 G, $A_H = 14.9$–15.2 G).[20]

20 a) K. Makino, H. Imaishi, S. Morinishi, T. Takeuchi, Y. Fujita, *Biochem. Biophys. Res. Commun.* **1986**, *141*, 381. b) Y. Yamakoshi, S. Sueyoshi, K. Fukuhara, N. Miyata, T. Masumizu, M. Kohno, *J. Am. Chem. Soc.* **1998**, *120*, 12363. c) Y. Yamakoshi, N. Umezawa, A. Ryu, K. Arakane, N. Miyata, Y. Goda, T. Masumizu, T. Nagano, *J. Am. Chem. Soc.* **2003**, *125*, 12803.

21 a) G. R. Buettner, *Free Radical Biol. Med.* **1987**, *3*, 259. b) W. Adam, S. Marquardt, D. Kemmer, C. R. Saha-Möller, P. Schreier, *Org. Lett.* **2002**, *4*, 225. c) P. Ionita, M. Conte, B. C. Gilbert, V. Chechik, *Org. Biomol. Chem.* **2007**, *5*, 3504.

22 P. Neta, R. E. Huie, A. B. Ross, *J. Phys. Chem. Ref. Data* **1990**, *19*, 413.

23 D. L. Mohler, J. R. Shell, J. G. Coonce, J. L. Mirandi, L. Riera, L. Cuesta, J. Pérez, *J. Org. Chem.* **2007**, *72*, 8755.

24 D. L. Mohler, J. R. Downs, A. L. Hurley-Predecki, J. R. Sallman, P. M. Gannett, X. Shi, *J. Org. Chem.* **2005**, *70*, 9093.